Electronic Supplementary Material (ESI) for Journal of Materials Chemistry A.

Electronic Supplementary Information (ESI) for

Mass production of biodegradable porous foam for simultaneous solar evaporation and thermoelectricity generation

Zhipeng Liu [a], Zhi Gong [a], Xiaolong Li [a], Jiaxin Ren [a], Jiang Gong [a,b,*], Jinping Qu [a,b], Ran Niu [a,b,*]

[a] Key Laboratory of Material Chemistry for Energy Conversion and Storage, Ministry of Education, Hubei Key Laboratory of Material Chemistry and Service Failure, Hubei Engineering Research Center for Biomaterials and Medical Protective Materials, Semiconductor Chemistry Center, School of Chemistry and Chemical Engineering, Huazhong University of Science and Technology, Wuhan 430074, China.

[b] National Engineering Research Center of Novel Equipment for Polymer Processing, Key Laboratory of Polymer Processing Engineering, Ministry of Education, Guangdong Provincial Key Laboratory of Technique and Equipment for Macromolecular Advanced Manufacturing, School of Mechanical and Automotive Engineering, South China University of Technology, Guangzhou 510641, China.

*Corresponding authors.

E-mail addresses: gongjiang@hust.edu.cn (J. Gong); niuran@hust.edu.cn (R. Niu)

Note S1 Characterization

The morphology of PHA-*x* was characterized by scanning electron microscope (SEM, SU8010). Water contact angle was recorded using micro-optical contact angle measurement (Dataphysics OCA15EC). Fourier transform infrared spectroscopy (FTIR, Thermo Fisher, USA) was performed to identify species and molecular interactions. Absorption spectrum was monitored using UV-vis-NIR spectrophotometer (Lambda 750 S, PerkinElmer, USA). The absorption is calculated as follows, Absorption = 1-Transmission - Reflection. The metal cation concentrations before and after absorption in the aqueous solution were analyzed by using an inductively coupled plasma optical emission spectrometer (ICP-OES, Agent 5110, USA).

Note S2 Solar steam and electricity generation

Interfacial solar evaporation in the laboratory was conducted at environmental temperature of 26±0.5 °C and relative humidity of 30±1%. Solar simulator (PLS-SXE300, Perfect Light, China) was used for solar irradiation, for which the energy density was regulated by a thermopile connected to an optical power meter (CEL-FZ-A CEAULIGHT, China). High precision electronic analytical balance (JA 2003, Soptop, accuracy=0.1 mg) was used to record real-time mass losses. The temperature profile of the sample surface was monitored by using an IR camera (DMI220, East America). The solar-to-vapor conversion efficiency (η, %) was calculated as below,

$$\eta = \frac{mh_{LV}}{3600I} \tag{S1}$$

where h_{LV} is the water evaporation enthalpy (kJ kg^{-1}), I is the energy of the input light (kW m^{-2}), and m is the evaporation rate (kg m^{-2} h^{-1}) after deducting that in the dark. For electric power generation, the whole device was composed of PHA-*x*, air-laid paper, and a TE module. The TE module (SP1848-27145) with a dimension of 4 cm × 4 cm × 0.3 cm was placed on a thermostatic plate connected to a low constant temperature bath (Powereach). Air-laid paper of the same size sandwiched between the TE module and the PHA-*x* foam was used for continuous water supply. The open-circuit voltage, sample upper surface temperature and short-circuit current were obtained by the data acquisition unit (Keysight 34972A).

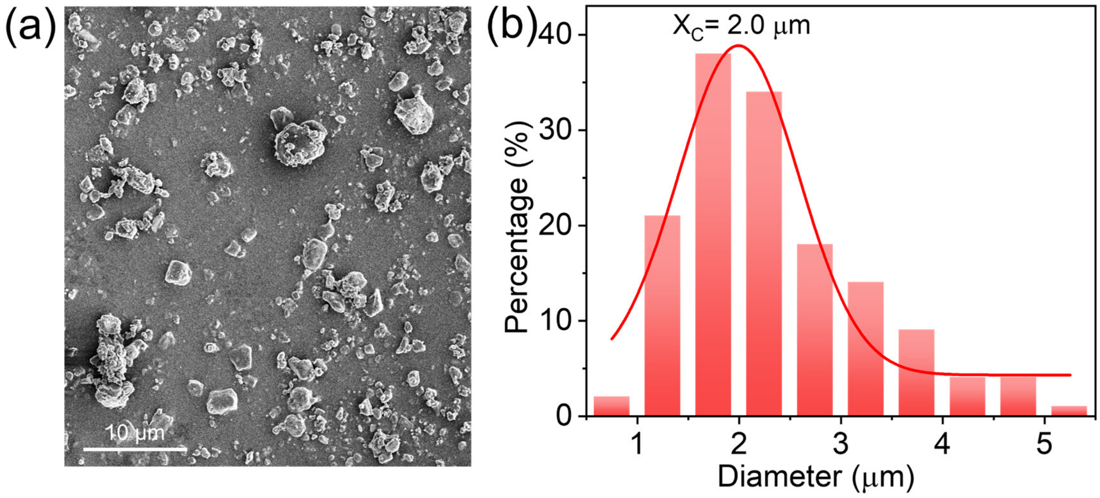

Fig. S1 Size distribution plot of the sugar cane after ball-milling.

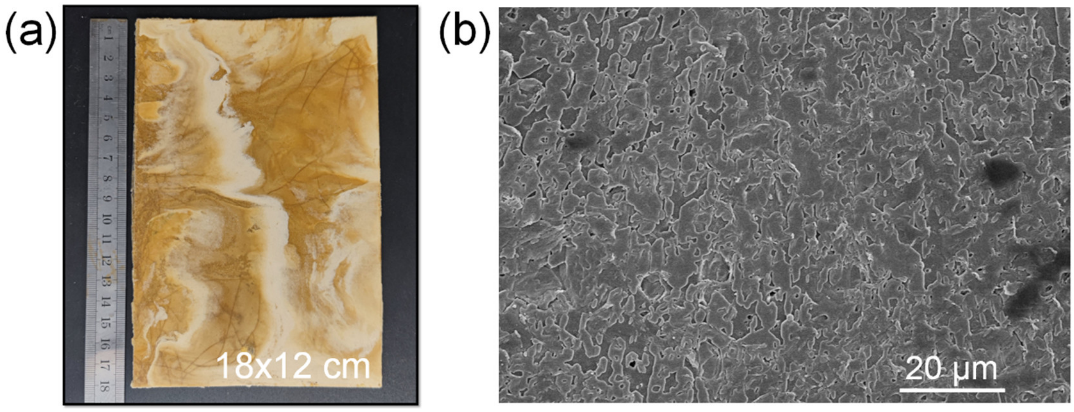

Fig. S2 (a) Photograph and (b) SEM image of PHA/cane sugar blend.

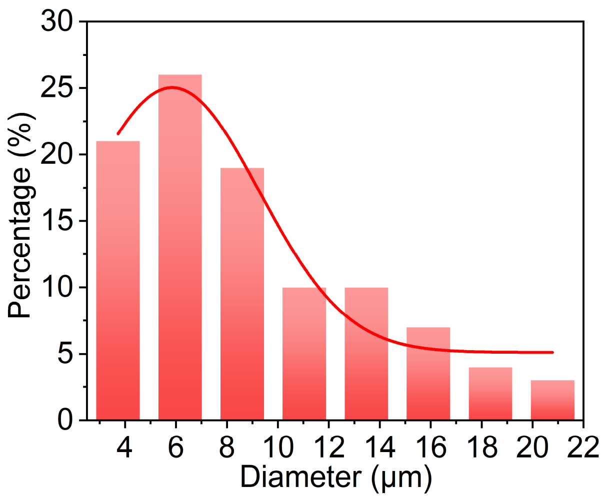

Fig. S3 Size distribution plot of the pore size in PHA-6 foam.

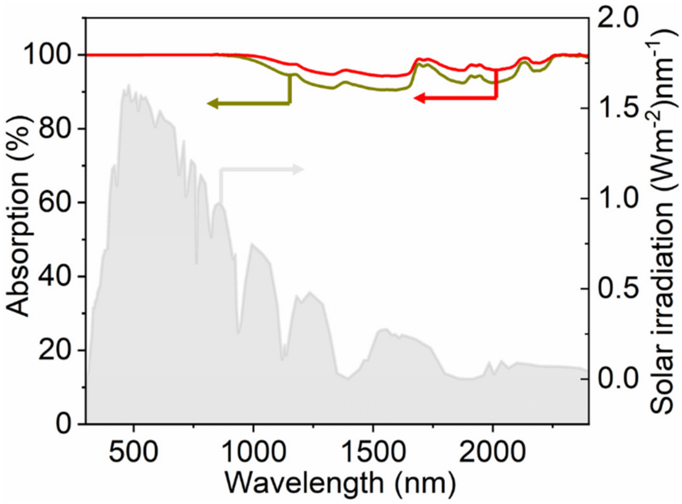

Fig. S4. Solar absorption spectra of PHA-3 and PHA-12.

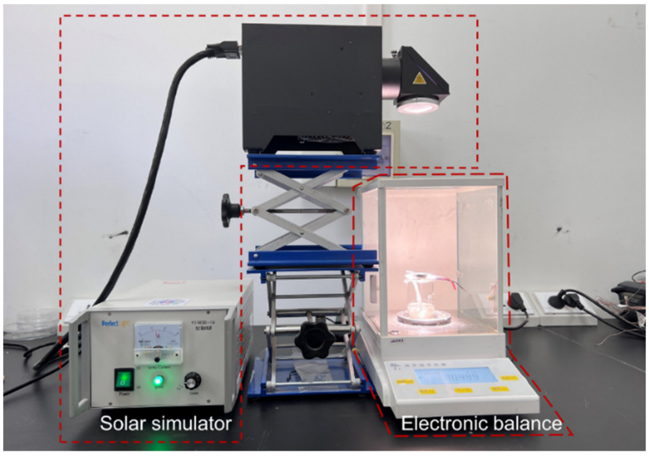

Fig. S5 Photograph of the solar water generation system used in this work.

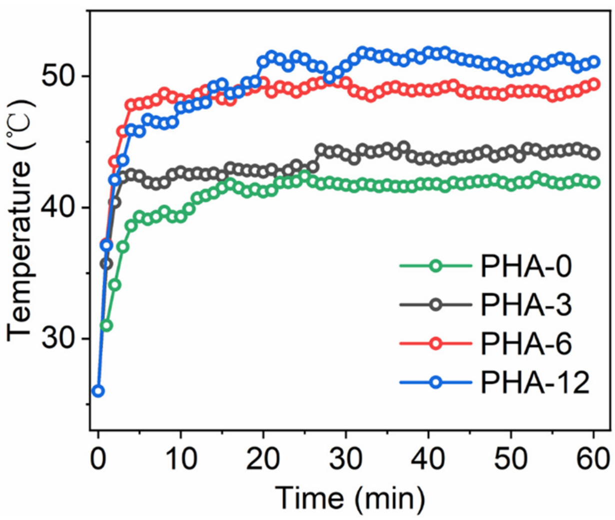

Fig. S6 Temperature versus time for PHA-*x* under solar irradiation of 1 Sun.

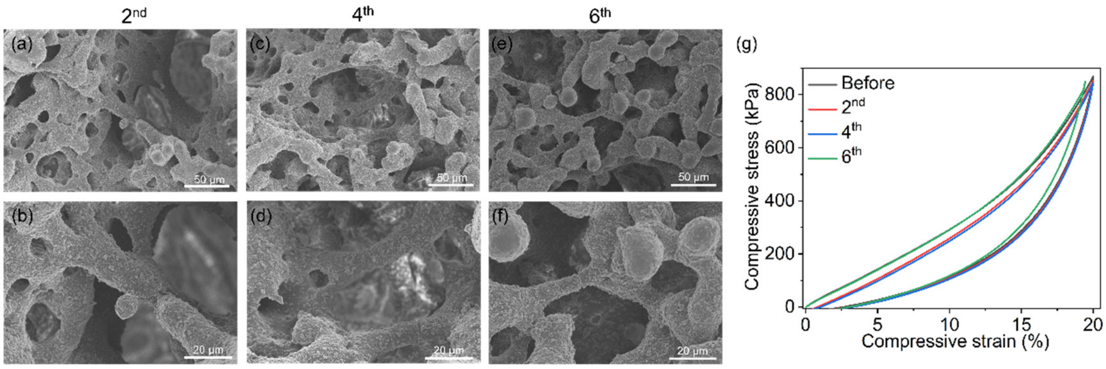

Fig. S7 (a-f) SEM images and (g) compressive stress-strain curves of PHA-6 foam after different cycles of solar irradiation.

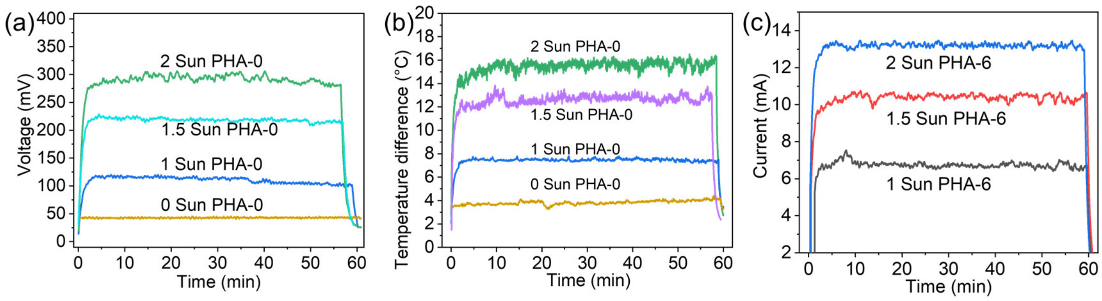

Fig. S8 (a) Open-circuit voltage and (b) surface temperature difference of PHA-0 under different intensities of solar irradiation. (c) Short-circuit current of PHA-6 under different intensities of solar irradiation.

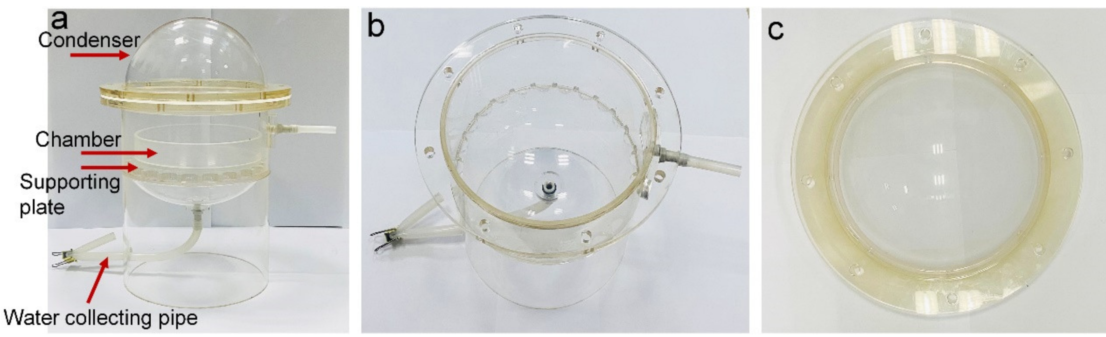

Fig. S9 (a-c) Photographs of the home-made setup for the outdoor solar evaporation experiment.

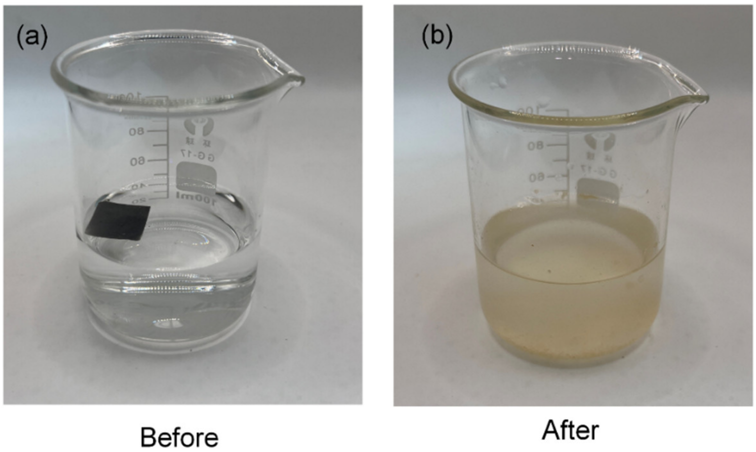

Fig. S10 Photographs of PHA-6 foam (a) before and (b) after being degraded in 10% NaOH solution for 24 h.

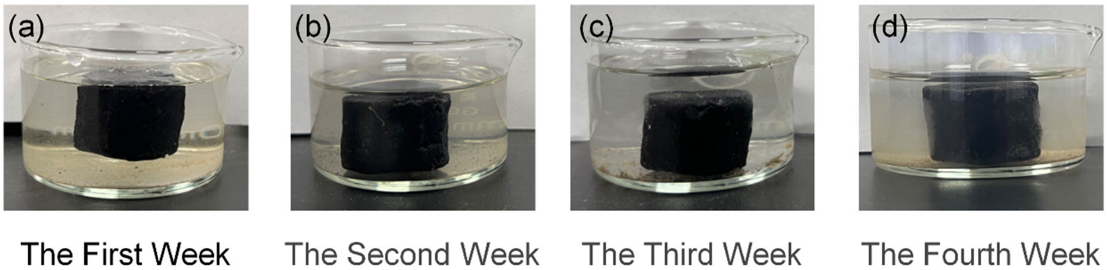

Fig. S11 (a-d) Images of PHA in unfiltered seawater for 4 weeks.

Table S1 Thermal conductivity of PHA-*x*.

Sample	Thermal conductivity (W m^{-1} K^{-1})
PHA-0	0.0877
PHA-6	0.0861

Note S3 Analyses of heat loss

Normally, during the process of solar steam generation, the heat loss consists of three components, i.e., radiation, convection and conduction. The calculation details are shown below.

(1) Radiation

The heat radiation loss was calculated by the Stefan-Boltzmann equation:

$$\phi = \varepsilon A\sigma(T_1^4 - T_2^4) \quad \text{(S2)}$$

where ϕ represents heat flux, ε is the emissivity (the value is 1), A is the effective evaporation surface area (530 mm^2), ε is the Stefan-Boltzmann constant (the value is 5.67×10^{-8} W m^{-2} K^{-4}), and T_1 is the surface temperature of evaporator after stable steam generation under one-sun illumination (ca. 49 °C, 322.15 K), and T_2 is the ambient temperature upward the surface of the evaporator (ca. 42 °C, 315.15 K). Therefore, the calculated heat radiation loss of PHA-6 is ca. 2.7%.

(2) Convection

The convective heat loss is defined by Newton' law of cooling:

$$Q = hA\Delta T \quad \text{(S3)}$$

where Q is the convection heat flux, h represents the convection heat transfer coefficient, which is approximately 5 W m^{-2} K^{-1} as reported, and ΔT is different between the surface temperature of PHA-6 and the ambient temperature upward the absorber. The calculated convective heat loss is about 2.1%.

(3) Conduction

$$Q = Cm\Delta T \quad \text{(S4)}$$

where Q is the heat energy, C represents the specific heat capacity of water (4.2 kJ $°C^{-1}$ kg^{-1}), m denotes the weight of water (g), and ΔT is the increased temperature of water. In this work, m = 50 g, ΔT = 1.2 °C. Consequently, according to Equation 4, the calculated conduction heat loss of PHA-6 is ca. 6.0%.

Therefore, the heat loss of PHA-6 in the water evaporation processes is 10.8%.

Note S4 Calculation of evaporation rate and conversion efficiency

The evaporation rate (m, kg m^{-2} h^{-1}) and solar-to-vapor energy conversion efficiency (η, %) were calculated by the following equations:

$$m = \Delta m/S \times t \quad \text{(S5)}$$

$$\eta = m' \times h\mathrm{Lv}/3600P\mathrm{in} \quad \text{(S6)}$$

where Δm is the mass change of water within 1 h (kg), S is the surface area of hydrogel evaporator (m^2), t is the time of solar irradiation (1 h), m' is the evaporation rate after subtracting the evaporation rate under dark condition (kg m^{-2} h^{-1}), h_{Lv} is the water vaporization enthalpy (J g^{-1}), and P_{in} is the intensity of light (1 kW m^{-2}).

Note S5 Evaporation in the dark for water evaporation enthalpy calculation

The evaporation rate was recorded to estimate the evaporation enthalpy of hydrogel samples by making a comparison with the known theoretical value of liquid water. The water evaporation enthalpy in hydrogels was calculated by the following equation:

$$U_{in} = E_0 m_0 = E_{equ} m_g \tag{S7}$$

where U_{in} is the energy achieved from the environment per hour; E_0 and m_0 refer to the theoretical water evaporation enthalpy (kJ g^{-1}) and the weight of water evaporation (g) within 1 h under dark condition, respectively; m_g means the weight of water evaporation (g) using hydrogel absorbers; E_{equ} is the equivalent evaporation enthalpy (kJ g^{-1}) of water in hydrogels.

Note S6 Calculation of heat loss, effective photothermal conversion efficiency and energy gain from ambient

During the solar-driven evaporation process, the temperature at the bottom of the PHA-6 foam is close to the room temperature. Therefore, the heat conduction from bottom of PHA-6 foam to the bulk water is negligible. Consequently, the heat loss of solar-driven evaporation mainly includes radiation and convection heat loss. The energy conservation of the PHA-6 foam can be descripted by

$$Q_{\mathrm{solar}} = Q_{\mathrm{evap}} + Q_{\mathrm{conv}} + Q_{\mathrm{rad}} \tag{S8}$$

and the effective photothermal conversion efficiency is expressed as

$$\eta_{\mathrm{photothermal}} = 1 - \frac{Q_{\mathrm{conv}} + Q_{\mathrm{rad}}}{Q_{\mathrm{solar}}} \tag{S9}$$

Where Q_{solar} is the total solar energy absorbed by PHA-6 foam. Q_{evap} is the effective energy utilized for evaporation. Q_{conv} and Q_{rad} represent the convection heat loss and radiation heat loss, respectively. The size of a typical PHA-6 foam sample is $\Pi \times r^2 \times h$ (3.14×1.3×3 cm^3). In the 3D foam evaporators, the evaporative surfaces include one top surface ($A_{top} = \frac{1}{2}\Pi r^2$) and side surfaces of sponges ($A_{side} = 2rh$). Moreover, the side surface has a temperature gradient ($T_{side}(b)$) as shown by Figure 4g. Q_{conv} and Q_{rad} can then be calculated by

$$Q_{\text{conv}} = A_{top}h_{\text{conv}}(T_{top} - T_\infty) + \int A_{side}h_{\text{conv}}(T_{side}(b) - T_\infty)\, d_b \quad \text{(S10)}$$

$$Q_{\text{rad}} = \alpha_{top}\sigma A_{top}(T_{top}^4 - T_\infty^4) + \alpha_{side}\sigma \int A_{side}(T_{side}^4(b) - T_\infty^4) d_b \quad \text{(S11)}$$

where h_{conv} is the convective heat transfer coefficient of 5 W m^{-2} K^{-1}. α and σ are the surface emissivity of PHA-6 foam (0.95) and Stefan-Boltzmann constant (5.670367×10^{-8} kg s^{-3} K^{-4}), respectively. T_∞ is the environmental temperature (303.15 K). $T_{side}(b)$ was measured by the FLIR infrared camera. Under one-sun solar illumination for 60 min, the convection heat loss and radiation heat loss were estimated to be 21.8 mW and 13.8 mW, respectively. The corresponding effective photothermal conversion efficiency was estimated to be 93.54%.

Based on the temperature difference between the evaporation surfaces and ambient environment, the ambient energy input through convection and radiation for the 3D sponges was calculated by the following equation,

$$Q_{\text{ambient}} = -4\int_{\mathrm{T_{side}(b)\le T_\infty}} A_{\text{side}}h_{\text{conv}}(T_{\text{side}}(b) - T_\infty)\, \mathrm{d_b} - 4\alpha_{\text{side}}\sigma \int_{T_{\text{side}}(b)\le T_\infty} A_{\text{side}}(T_{\text{side}}^4(b) - T_\infty^4)\, \mathrm{d_b} \quad \text{(S12)}$$

$$\eta_{\text{ambient}} = {Q_{\text{ambient}}}/{Q_{\text{solar}}} \quad \text{(S13)}$$

Where η_{ambient} is the percentage of ambient energy input for the sponges during the solar-thermal evaporation. Under one-sun solar illumination for 60 min, the ambient energy input and the corresponding efficiency were estimated to be 33.75 mW and 6.36%, respectively.

Table S2 Comparison of evaporation rate and power density values of various hybrid devices under 1 kW m^{-2} irradiation.

Entry	Photothermal material	Evaporation rate (kg m^{-2} h^{-1})	Power density (W m^{-2})	Reference in ESI
1	PHA-6	2.26	0.76	This work
2	Carbon nanotube modified	1.1	0.5	[1]

	filter paper			
3	MoS_2-based composites	1.52	9×10^{-4}	[2]
4	W-doped VO_2 PVDF membrane	1.39	1.0×10^{-4}	[3]
5	3D porous carbon foam	1.37	0.48	[4]
6	Cu-MOF coated membrane	2.07	1.8×10^{-2}	[5]
7	3D Asymmetric evaporator	1.93	6×10^{-7}	[6]
8	Coupling of TGC and RED	1.4	1.11	[7]
9	broadband semiconductor foam	1.29	0.175	[8]
10	Au@Bi_2MoO_6-carbon dot	1.69	0.974	[9]
11	MnO/C nanoparticle	2.38	0.77	[10]

Table S3 The calculation of the cost of PHA-6.

Material	Cost	Remarks
PHA	¥0.2 g^{-1}	It is obtained from Zhuhai Meda Technology Co. Ltd
Cane sugar	¥0.054 g^{-1}	It is obtained by Sinopharm Chemical Reagent Co. Ltd. China
TA	¥0.714 g^{-1}	It is obtained from Shanghai Maclin Biochemical Technology Co. LTD
APTES	¥0.576 g^{-1}	It is obtained from Shanghai Aladdin Biochemical Technology Co. Ltd.
Tris	¥0.779 g^{-1}	It is obtained from Shanghai Aladdin Biochemical Technology Co. Ltd.
$Fe_2(SO_4)_3$	¥0.172 g^{-1}	It is obtained by Sinopharm Chemical

		Reagent Co. Ltd. China.
PHA-6 (10 × 8 cm^2)	¥ 1.188 per piece	In this process, 2.25 g PHA, 9 g Cane sugar, 0.1125 g TA, 0.1125 g APTES, 0.0675 g Tris, 0.225 g $Fe_2(SO_4)_3$, and 850 mL water are needed. The cost for the electricity and equipment is estimated as ¥ 0.5.

References in ESI

[1] P. Yang, K. Liu, Q. Chen, J. Li, J. Duan, G. Xue, Z. Xu, W. Xie and J. Zhou, *Energy Environ. Sci.*, 2017, **10**, 1923.

[2] Z. Guo, J. Wang, Y. Wang, J. Wang, J. Li, T. Mei, J. Qian and X. Wang, *Chem. Eng. J.*, 2022, **427**, 131008.

[3] M. Jiang, Q. Shen, J. Zhang, S. An, S. Ma, P. Tao, C. Song, B. Fu, J. Wang, T. Deng and W. Shang, *Adv. Funct. Mater.*, 2020, **30**, 1910481.

[4] X. Liu, D.D. Mishra, Y. Li, L. Gao, H. Peng, L. Zhang and C. Hu, *ACS Sustain. Chem. Eng.*, 2021, **9**, 4571-4582.

[5] X. Ma, Z. Li, Z. Deng, D. Chen, X. Wang, X. Wan, Z. Fang and X. Peng, *J. Mater. Chem. A*, 2021, **9**, 9048.

[6] J. Liu, J. Gui, W. Zhou, X. Tian, Z. Liu, J. Wang, J. Liu, L. Yang, P. Zhang, W. Huang, J. Tu and Y. Cao, *Nano Energy*, 2021, **86**, 106112.

[7] H. Wang, W. Xie, B. Yu, B. Qi, R. Liu, X. Zhuang, S. Liu, P. Liu, J. Duan and J. Zhou, *Adv. Energy Mater.*, 2021, **11**, 2100481.

[8] H. Jiang, L. Ai, M. Chen and J. Jian, *ACS Sustain. Chem. Eng.*, 2020, **8**, 2168-0485

[9] Z. Zheng, H. Li, X. Zhang, H. Jiang, X. Geng, S. Li, H. Tu, X. Cheng, P. Yang and Y. Wang, *Nano Energy*, 2020, **68**, 104298.

[10] Z. Fan, J. Ren, H. Bai, P. He, L. Hao, N. Liu, B. Cheng, R. Niu and J. Gong, *Chem. Eng. J.*, 2023, **451**, 138534.